

Osteological and Molecular Identification of Brucellosis in Ancient Butrint, Albania

Michael J. Mutolo, Lindsey L. Jenny, Amanda R. Buszek, Todd W. Fenton, and David R. Foran*

Michigan State University, East Lansing, MI 48824

KEY WORDS brucellosis; *Brucella* spp.; ancient DNA; cavitating lytic vertebral lesions

ABSTRACT Ancient skeletal remains can harbor unique information about past civilizations at both the morphological and molecular levels. For instance, a number of diseases manifest in bone, some of which have been confirmed through DNA analysis, verifying their presence in ancient populations. In this study, anthropological analysis of skeletal remains from the ancient Albanian city of Butrint identified individuals with severe circular lytic lesions on their thoracic and lumbar vertebrae. Differential diagnosis suggested that the lesions resulted from pathologies known to affect these skeletal regions, such as tuberculosis (TB) or brucellosis. Relevant bones of two adolescent males from the 10th to 13th century AD that displayed the lesions, along with unaffected individuals, were collected in the field. Genetic screening of the

skeletal samples for TB was repeatedly negative, thus additional testing for *Brucella* spp.—bacteria of livestock and the causative agent of brucellosis in humans—was conducted. Two *Brucella* DNA markers, the *IS6501* insertion element and *Bcsp31* gene, amplified from the affected vertebrae and/or ribs, whereas all unaffected individuals and control samples were negative. Subsequent DNA sequencing confirmed the presence of the brucellar *IS6501* insertion element. On the basis of the skeletal lesions, negative tests for TB, and positive *Brucella* findings, we report a confirmed occurrence of brucellosis in archaeologically recovered human bone. These findings suggest that brucellosis has been endemic to the area since at least the Middle Ages. *Am J Phys Anthropol* 000:000–000, 2011. © 2011 Wiley Periodicals, Inc.

A major goal of physical anthropologists and paleopathologists is to understand the manifestation of disease in past individuals and societies. Traditionally, such studies involve evaluation of ancient skeletal remains, utilizing techniques including gross analysis, X-ray examination, chemical tests, and microscopic assessments. These techniques have proven useful in recognizing potential pathogens that cause skeletal pathologies; however, such techniques can be limited by the condition of the remains themselves or in their ability to identify a definitive disease agent. In addition, different types of pathogens can produce similar bone pathologies. A novel approach has been developed to help circumvent these problems, wherein osteological methods are combined with molecular analyses to not only characterize the disease process, but also identify the specific pathogen based on its DNA endurance in bone.

Molecular identification of pathogens in skeletal or mummified remains is possible via the polymerase chain reaction (PCR), in which small amounts of DNA are copied *in vitro*. Generally, osteological analyses are conducted to generate a list of potential causative agents of the skeletal pathologies through differential diagnosis. Next, PCR-based tests are utilized to preferentially target pathogen genomic or plasmid DNA. Successful DNA amplification is considered a sign of either acute or chronic infection during an individual's lifetime. This methodology has been used to identify a range of diseases in ancient societies, including malaria, leprosy, plague, syphilis, and tuberculosis (TB) (Mays et al., 2001, 2002; Hershkovitz et al., 2008; Raoult, 2008). Of these, TB, which results from respiratory or gastrointestinal infection by small, acid-fast, gram-positive bacterial members of the *Mycobacterium tuberculosis* (MTB) complex, has been identified most frequently. The complex includes *M. tuberculosis*, *Mycobacterium bovis*, *Mycobacterium microti*, and *Mycobacterium africanus*, which infect a wide range of hosts. Human disease is usually caused by *M. tuberculosis* or *M. bovis* and is contracted through inhalation of contaminated aerosol or ingestion of infected meat or dairy products (Ortner, 2003).

Although TB is primarily a respiratory disease, secondary infection can occur in a number of organs and tissues, including bone. The most common site of skeletal involvement is the vertebral column (Ortner, 2003). It is thought that the bacilli travel through the bloodstream, up the paravertebral plexus, and attack the center, anterior surface (paradiscal region) of the vertebral body. Uhlinger (1970) undertook a study of 62 individuals diagnosed with TB at autopsy and found the most common vertebrae involved were thoracic (T6–T12) and lumbar (L1–L5). Vertebral TB infection is generally lytic, producing circular resorption lesions on the anterior surface of the vertebral body (Mays et al., 2002). The bacteria continue to cause lesions and degradation until the vertebrae collapse, resulting in kyphosis, or angling of the vertebral column followed by fusion of the spine, a condition known as Pott's disease. Extra-vertebral TB also affects the skull, ribs, pelvis, and bones of the limbs (Steinbock, 1976; Ortner, 2003).

Although TB is primarily a respiratory disease, secondary infection can occur in a number of organs and tissues, including bone. The most common site of skeletal involvement is the vertebral column (Ortner, 2003). It is thought that the bacilli travel through the bloodstream, up the paravertebral plexus, and attack the center, anterior surface (paradiscal region) of the vertebral body. Uhlinger (1970) undertook a study of 62 individuals diagnosed with TB at autopsy and found the most common vertebrae involved were thoracic (T6–T12) and lumbar (L1–L5). Vertebral TB infection is generally lytic, producing circular resorption lesions on the anterior surface of the vertebral body (Mays et al., 2002). The bacteria continue to cause lesions and degradation until the vertebrae collapse, resulting in kyphosis, or angling of the vertebral column followed by fusion of the spine, a condition known as Pott's disease. Extra-vertebral TB also affects the skull, ribs, pelvis, and bones of the limbs (Steinbock, 1976; Ortner, 2003).

Grant sponsor: Butrint Foundation, Packard Humanities Institute.

*Correspondence to: David Foran, 560 Baker Hall, Michigan State University, East Lansing, MI 48824. E-mail: foran@msu.edu

Received 15 July 2011; accepted 22 October 2011

DOI 10.1002/ajpa.21643
Published online in Wiley Online Library
(wileyonlinelibrary.com).

In 2001, Mays et al. reported their examination of nine skeletons from the Wharram Percy Collection. Initial gross and X-ray analyses showed that several of the individuals had TB-consistent lytic lesions, along with vertebral body collapse and kyphosis. However, the authors noted that a number of other pathologies could have caused the lesions, including malignant neoplastic disease, trauma, or brucellosis, thus they were hesitant to declare TB as the causative agent without confirmation. DNA was extracted and amplified from vertebrae of each individual, and screened for three markers specific to the MTB complex: *IS6110*, the *oxyR* pseudogene, and the *mtp40* pseudogene. *IS6110* is a mobile insertion element present in 8–20 copies in most members of the MTB complex, including the causative agents of TB, whereas *oxyR* and *mtp40* have been utilized to help differentiate *M. tuberculosis* and *M. bovis*. Bones from seven of the nine individuals generated positive results, confirming that MTB complex DNA was present. Mays et al. (2001) also screened for *Brucella* spp. DNA and obtained negative results.

Brucella spp. pathogens can produce skeletal lesions similar to TB, and the two infections can potentially be differentiated and confirmed in ancient skeletal remains using DNA-based methodologies. *Brucella* spp. are gram-negative coccobacilli that cause respiratory inflammation and reproductive failure in livestock (Acha and Szyfres, 1980). The bacteria also produce a zoonotic infection in humans (brucellosis), which was first identified in the 19th century by surgeon Sir David Bruce. During examination of suspected malaria cases in the Malta Garrison, Bruce found that some deaths were caused by a novel organism, *Brucella melitensis* (Aufderheide and Rodriguez-Martin, 1998). Although *B. melitensis* remains the most common causative agent of brucellosis in humans, infection by *Brucella abortus*, *Brucella ovis*, and *Brucella suis* are also possible (Pappas et al., 2006). Human *Brucella* spp. infection is usually acquired through ingestion of infected meat or dairy products and includes an incubation period ranging from 3 weeks to several months before onset of the disease. Primary infection typically manifests as chronic respiratory illness and fever, whereas secondary infection of skeletal tissue can occur when the bacteria become systemic and spread to cancellous bone.

Clinical reports suggest that skeletal involvement occurs in 20–85% of brucellosis cases (Geyik et al., 2002). *Brucella* spp. infection can cause spondylitis in the lumbar and thoracic spine, osteomyelitis in long bones and the pelvis, and arthritis (Ariza et al., 1985; Kelly et al., 1960). Vertebral infection begins in the intervertebral disc followed by “mild osteoporosis of the contiguous vertebrae, leading to anterior vertebral plate erosions” (Glasgow, 1976). A healing phase often follows, resulting in “dense sclerosis of the involved bone and the appearance of the so-called “parrot-beak” osteophyte” (Glasgow, 1976). Vertebral *Brucella* spp. infection can display either a focal or diffuse pattern. The former involves only one vertebra, with lesions occurring primarily along its superior edge, whereas a diffuse pattern shows lesions throughout a vertebra, with infection spreading to adjacent vertebrae or intervertebral disks (Sharif et al., 1989). Radiological studies of brucellosis indicate that it is more likely to involve the anterior surface of the vertebral body (Turunc et al., 2007). Epiphysitis of the antero-superior corner of the lumbar vertebrae, often referred to as the Pedro-Pons’ sign, is commonly used to

diagnose the disease in clinical cases (Ariza et al., 1985; Karabay et al., 2007).

In spite of these standard disease markers in bone, brucellosis remains difficult to diagnose clinically due to variability in skeletal manifestation. Given this, molecular methods have been developed to screen for the genus (Ouahrani et al., 1993; Bricker, 2002), which is generally identified using the *IS6501* insertion element (aka *IS711*) and/or the *Bcsp31* gene. *IS6501* is a multi-copy locus present in various *Brucella* species, including those that infect humans. *Brucella* spp. average 5–15 copies of the element, with some species having as many as 30 copies (Ouahrani et al., 1993). *Bcsp31* encodes an immunogenetic membrane protein, and is specific to infectious members of the genus. The presence of either marker in DNA extracted from skeletal material directly indicates that the individual suffered from brucellosis.

In this study, human skeletons from ancient Albania were examined. Osteological analyses identified skeletal lesions consistent with various diseases, including TB and brucellosis. Molecular methods were used to screen skeletal DNA for genomic or plasmid DNA of the MTB complex and *Brucella* spp. Identification of the causative agent of the lesions allows for an increased understanding of how such diseases can be diagnosed in skeletal remains and also provides novel information about this important geographic region and its past inhabitants.

MATERIALS

The skeletal material used in this study came from the ancient Albanian city of Butrint (ancient Buthrotum), which is located on a small peninsula in southwest Albania. The city is largely surrounded by the waters of Lake Butrint and the Vivari Channel, which drain into the Ionian Sea. Butrint, along with the Greek island of Corfu, was valued from Hellenistic times to the Napoleonic Wars as a port and strategic base dominating the narrow Straits of Corfu. The city has a rich history, being founded as an early Hellenistic sanctuary, developing into a large Roman colony, and then flourishing as an early Christian center. Throughout its final centuries, Butrint served as an outpost of the Byzantine Empire and a fortified Venetian market town until it was abandoned in the late Middle Ages due to flooding. This elaborate progression is reflected in the array of monuments preserved at the site, including a 4–2nd century BC theatre, a late Roman residence (the Triconch Palace), an adjacent Roman Merchant’s House, the Christian Junia Rufina Well, and a Christian baptistery dating from the 6th century AD. The Roman colony at Butrint expanded across the Vivari Channel, producing a suburb on the Vrina Plain. On the east shore of Lake Butrint is Diaporit, the site of a luxurious Hellenistic–Roman period villa laid out in terraces covering over 2,000 m², which was reused in the late 5th century AD by a monastic community centered on a large Christian pilgrimage church. In 1992, Butrint was designated a UNESCO World Heritage Site, and since that time extensive archaeological excavations and analyses, as well as anthropological studies, have been conducted by the Butrint Foundation in partnership with the Albanian Institute of Archaeology (UNESCO, 1999).

Osteological methods

During the excavations of Butrint and Diaporit, numerous graves containing human skeletal remains were located. Anthropologists from Michigan State University have examined the remains of 48 individuals from Butrint and 26 individuals from Diaporit. Biological profiles were developed for each, including sex, age, and associated dental and skeletal pathologies. Adults were aged using methods appropriate for the preservation of each individual, such as pubic symphysis phases (Suchey and Katz, 1998), auricular surface (Lovejoy et al., 1985), and sternal rib ends (Işcan et al., 1984, 1985). Subadults were aged using dental development and epiphyseal union (Ubelaker, 1984; Scheuer and Black, 2004). Sex was estimated based on cranial and pelvic morphology (Phenice, 1969; Buikstra and Ubelaker, 1994).

Skeletal pathologies were recorded following gross examination. Initial examinations identified five skeletons that showed signs of pathology consistent with various disease processes (Table 1). Two of these (Burials 2272 and 4015) were located at the Butrint site and dated to the 10–13th century AD. No radiocarbon dates are available for these burials, however radiocarbon dates for two individuals in the same burial group as 4015 produced a range of AD 1020–1260. On the basis of site stratigraphy, 4015 appears to have been buried after these individuals (Bowden and Hedges, 2011). Burial 2272 was dated to the 10–12th centuries based on stratigraphy and pottery fragments mixed in the grave fill (Integrated Archaeological Database, 2011). Both 2272 and 4015 had similar cavitating lytic vertebral lesions (Figs. 1 and 2), and samples were collected for molecular analysis. Although radiological examination was not possible on site, sampled vertebrae from Burials 2272 and 4015 were X-rayed at Michigan State University.

Additional samples from three 5th to 7th century AD burials exhibited other skeletal pathologies (Table 1). These included Burial 213, an adult male from Diaporit that displayed extensive enthesopathic activity throughout the skeleton, Burial 319, an adult female from Diaporit who had osteophytic changes in the vertebrae, lesions on the parietals of the skull, and expansion of long bones, and Burial 5010, an adult female from Butrint, exhibiting circular erosive lesions on the skull and extensive periosteal reaction in various long bones. Finally, control samples were collected from two individuals from Diaporit that showed no skeletal pathologies (Burials 10 and 584).

Molecular methods

Vertebrae, rib fragments, and long bone sections from skeletons were transported to the Michigan State University Forensic Biology Laboratories for DNA analysis. No previous work on MTB complex or *Brucella* spp. DNA had been conducted in any of the laboratories utilized for this research, and DNA extraction, DNA amplification, positive control DNA setup, and real-time PCR were all conducted in separate laboratories. A thoracic or lumbar vertebra, rib fragment, and femur section (or ulna or tibia fragments if femora were absent) were analyzed for each burial. DNA extraction and analyses were conducted a minimum of three times for each bone. Digestion buffer (50 mM EDTA, 0.5% SDS, and 20 mM Tris pH 8.0) and water were sterilized by passage through a 0.22- μ m filter. A Dremel tool (Dremel Corpora-

tion; Racine, WI), sanding wheel, and 1.6 mm (1/16 inch) drill bits were scrubbed with a detergent/bleach mixture. Digestion buffer, water, Dremel tool, drill accessories, and consumables (1.5 ml tubes, pipet tips, PCR tubes, etc.) were autoclaved as appropriate, and UV irradiated to 6 J/cm². Bones were processed in a Clean Spot PCR/UV Workstation (Coy Lab Products; Grass Lake, MI). Ribs and long bones were sampled in regions that displayed porosity, lesions, or cortical expansion. Vertebrae were sampled directly from the center of the vertebral body, either close to the anterior surface or near the neural arch. A small region of the bone was washed by flushing the surface with 1–2 ml of digestion buffer, swabbing the area clean, and allowing it to air-dry. This region was gently sanded with a drill bit until white cortical material was revealed, followed by a second wash to remove residual bone powder. Twenty-five to 50 mg of new bone powder was generated by drilling into the cleaned region and collected in a 1.5 ml microcentrifuge tube. Five hundred microliters of digestion buffer and 5 μ l of proteinase K (20 mg/ml) were added to the bone powder. Reagent blanks, containing all reagents except bone powder, were prepared for each extraction. Samples and associated reagent blanks were incubated at 55°C overnight.

DNA extraction. A standard organic method was used to extract DNA from digested bone. An equal volume of phenol was added to each digest, followed by vortexing and centrifugation at 20,000g for 5 min. The aqueous layer was transferred to a new sterile 1.5 ml tube and two or three chloroform extractions (depending on the amount of color in the aqueous layer) were conducted using the same procedure. The aqueous layer was passed through a Microcon YM-10 filter device (Millipore; Billerica, MA) at 10,000g. The column was washed three times using 300 μ l of sterile 10 mM Tris, and 1 mM EDTA pH 8.0 (TE). DNA was eluted from the column with 20 μ l of sterile TE. A 1:10 dilution of the DNA was made using sterile TE for subsequent PCR reactions. Reagent blanks were processed in the same manner. DNAs were stored at –20°C.

Mitochondrial DNA amplification and sequencing. Mitochondrial DNA hypervariable region I (mtDNA HVI) amplification and sequencing was attempted from bones to assess if DNA was present. A PCR mastermix included: 2 μ l of Hot Master Taq buffer (Eppendorf North America; Westbury, NY), 0.3 μ l of 30 μ g/ μ l bovine serum albumin, 2 μ l of 2 mM deoxynucleotide 5'-triphosphates, 0.4 μ l of 20 μ M forward and reverse primer, and 1 unit of Hot Master Taq (Eppendorf North America) brought to a final volume of 19 μ l with sterile water. One microliter of diluted bone DNA was added to 19 μ l of mastermix. Amplification was conducted with an initial denaturation of 94°C for 5 min, thirty-five cycles of 94°C for 30 s, 56°C for 1 min, 72°C for 1 min, and a 72°C final extension for 7 min. Four microliters of the PCR products from initial amplifications were electrophoresed on a 3% agarose gel and visualized using ethidium bromide. Reactions that resulted in a faint or nonvisible product were amplified for an additional 10–15 cycles using a nested forward primer. Primer sequences were: HV1 F15989 (5'-ccatgcttacaagcaagt-3'), HV1 R16207 (5'-acttgcttgaagcatgggg-3'), nested primer HV1 F16057 (5'-aagtattgactcacccatca-3'). Amplifications were again visualized on a 3% agarose gel. Ten microliter sequencing reactions were prepared containing 4 μ l DTCS Quick

TABLE 1. Summary of paleopathologies observed in skeletal material used for molecular analysis^a

Skeleton	Vertebra	Rib	Long bone	Additional
BUT 2272	T3-T12, 1, L2, L4 contain cavitating lesions. Sacrum has bilateral lesions just posterior to auricular surface	Parietal surface shows cortical expansion and macroporosity	Femora: Sclerotic reactive bone on necks and posterior distal shafts (superior to condyles) Tibiae: Diaphyses and distal metaphyseal region show periosteal expansion Fibulae: Distal metaphyses show periosteal expansion; rounded appearance	Porotic hyperostosis on right parietal
BUT 4015	T3-T12, L1, L2 contain cavitating lesions. Sacrum has bilateral retro-auricular lesions	Parietal surface shows some cortical expansion and porosity	Femora: Sclerotic reactive bone on necks and posterior distal shafts (superior to condyles) Tibiae: Distal metaphyses show periosteal expansion; rounded appearance	None
DIAP 213	Lumbar osteophytic lipping	None	Femora: Left bone expanded with sclerotic reactive bone at proximal and distal ends Tibiae: Left bone expanded with sclerotic reactive bone at proximal and distal ends Ulna: Porotic lesions with sclerotic reactive bone at proximal and distal end	Extensive enthesopathic activity throughout skeleton
DIAP 319	Cervical osteophytic lipping	Parietal surface shows some porosity	Tibiae: Cortical expansion; reactive woven bone Fibulae: Cortical expansion; reactive woven bone	Skull: Lesions located on parietals
BUT 5010	Cervical osteophytic lipping	None	Femora: Periosteal reaction on left and right diaphyses Tibiae: Left tibia has healed cut marks; periosteal reaction on left and right diaphyses Fibulae: periosteal reaction on left and right diaphyses	Skull: Circular lesions located on parietals and frontal. Button osteoma on occipital None
Controls				
DIAP 10				
DIAP 584				

^a Skeletons are designated by location (DIAP: Diaporit; BUT: Butrint) and burial number.

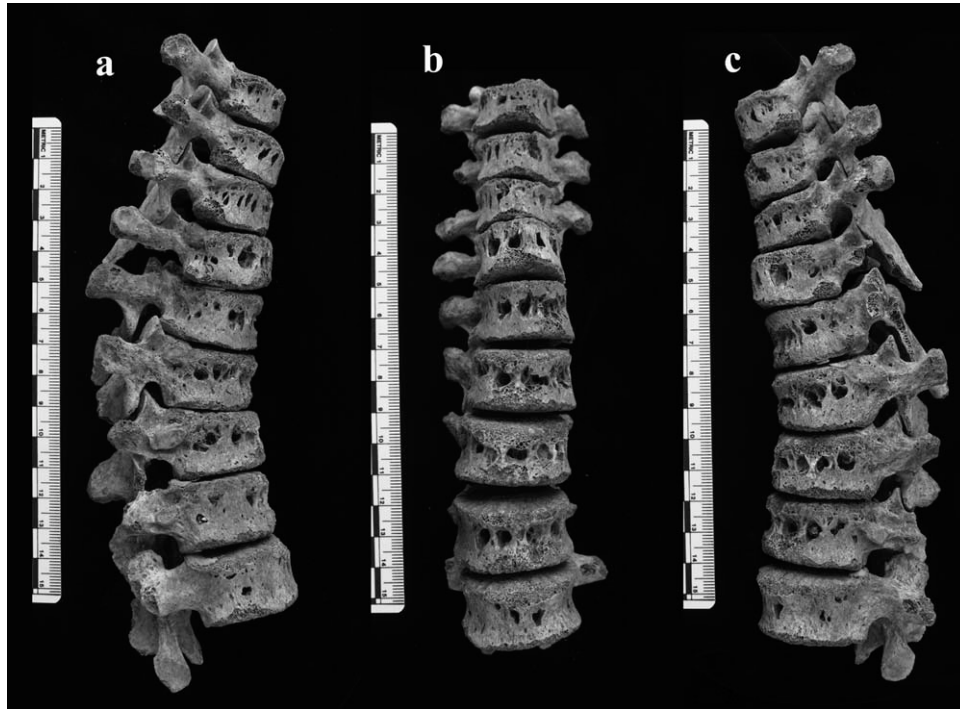


Fig. 1. Vertebrae from Butrint Burial 2272, a 17–21-year-old male. Displayed are T4–T8, T10–T12, and L1. (a) Right lateral aspect; (b) anterior aspect; (c) left lateral aspect.

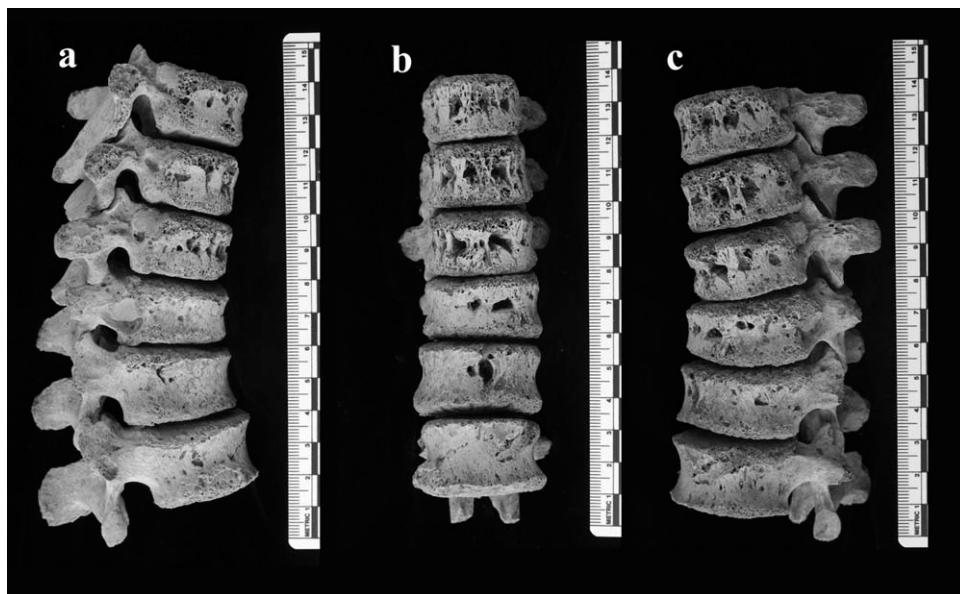


Fig. 2. Vertebrae from Butrint Burial 4015, a 17–21-year-old male. Displayed are T8, T9, T11, T12, L1, and L2. (a) Right lateral aspect; (b) anterior aspect; (c) left lateral aspect.

Start reagent (Beckman Coulter Inc.; Fullerton, CA), 1 μ l of either 20 mM forward or reverse primer, and \sim 6 ng of DNA template. Sequencing parameters consisted of denaturation at 96°C for 20 s, primer annealing at 50°C for 20 s, and elongation at 60°C for 4 min for 30 cycles. Sequencing reactions were electrophoresed on a CEQ™ 8000 Genetic Analysis System (Beckman Coulter Inc.) using the following parameters: capillary temperature 50°C, denature at 90°C for 120 s, inject at 2.0 kV for 15

s and separate at 4.2 kV for 60 min. Data were analyzed using the Beckman CEQ™ Sequencing Analysis software.

Real-time PCR. DNA sequences specific to the MTB complex (*IS6110*, *OxyR* and *Mtp40*) and *Brucella* spp. (*IS6501* and *Bcsp31*) were obtained from the NCBI Website [Sequence Accession No: *IS6110* (X17348), *OxyR* (AF313461), *Mtp40* (M57952), *IS6501* (M94960), and

Bcsp31 (M20404)]. Primer Express[®] software (Applied Biosystems; Foster City, CA) was used to design primer pairs, which included: *IS6110* (Forward 5'-gcttagcggcg-gacaa-3', Reverse 5'-gccgacgcggtcttataaa-3'; 62 bp), *OxyR* (Forward 5'-gcgacgaatcggtttgg-3', Reverse 5'-gcaagacgctgtaggacttct-3'; 63 bp), *Mtp40* (Forward 5'-cggcgaaatgacaatgca-3', Reverse 5'-ggtccggtggcattcgt-3'; 65 bp), *IS6501* (Forward 5'-cgcgcggtggattgac-3', Reverse 5'-agcggttaggccgatagca-3'; 58 bp), and *Bcsp31* (Forward 5'-gcgttgggagcagctt-3', Reverse 5'-ccagtccgatacggaaa-3'; 59 bp). Real-time PCR primer concentrations were optimized according to the SYBR[®] Green PCR Mastermix Protocol (Applied Biosystems, 2006). Optimum concentrations (nM Forward:Reverse) were *IS6110* (300:300), *OxyR* (900:300), *Mtp40* (300:900), *IS6501* (900:900), and *Bcsp31* (900:900).

Twenty-five microliter real-time PCR reactions were prepared using 12.5 μ l of 2 \times SYBR[®] Green PCR Mastermix (Applied Biosystems), 2.5 μ l of (optimized) forward and reverse primer, and 7.5 μ l sterile water. Two and a half microliters of extracted DNA or 1:10 diluted DNA were added to duplicate reactions. Up to five negative controls positioned across the thermal cycler, reagent blanks, and appropriate positive controls were run with each experiment. Positive control reactions contained approximately 10 genomic copies of either *M. bovis* or *B. abortus* DNA. As stated, all positive control amplifications were prepared in a separate laboratory.

Real-time PCR was conducted on an ABI 7000 Prism (Applied Biosystems) using the following parameters: initial 50°C hold for 2 min, a 10 min 95°C hold and 50 cycles of 95°C denaturation for 15 s, and a 1 min annealing/extension step at 60°C. A dissociation curve was generated by ramping the reactions from 64°C to 95°C. Amplification plots and dissociation curves of bone DNAs that amplified were compared to those of positive controls to assess consistency with MTB complex or *Brucella* spp. DNA. DNAs that amplified were electrophoresed on a 4% agarose gel and visualized using ethidium bromide.

Pyrosequencing. Twenty-five microliter PCR reactions of the DNA extracted from Burials 2272 and 4015 were prepared as described above, using AmpliTaq Gold[®] DNA polymerase (Applied Biosystems) and a single biotinylated *IS6501* forward or reverse primer. Cycling parameters included a 10 min 94°C hold, and 40 cycles of 94°C denaturation for 15 s, and a 1 min annealing/extension step at 60°C. Pyrosequencing was conducted on a PyroMark[®] Q24 Pyrosequencer (Qiagen; Germantown,

MD) with a PyroMark[®] Q24 vacuum workstation in SQA mode according to the manufacturer's instructions, utilizing Streptavidin[™] Sepharose High Performance Beads (GE Healthcare; South San Francisco, CA). Data were analyzed using PyroMark[®] Q24 Software 2.0.6. Sequences were searched using Basic Local Alignment Search Tool (BLAST; <http://blast.ncbi.nlm.nih.gov/Blast.cgi>), with nucleotide blast criteria of database "others" and "nucleotide collection," and optimized for "highly similar sequences".

RESULTS

Osteological analyses

Burial 2272 contained the remains of a 17–21-year-old male from the 10th to 12th century AD, whereas Burial 4015 contained the remains of a 17–21-year-old male from the 12th to 13th century AD. Both individuals displayed cavitating lytic lesions in the thoracic and lumbar vertebrae, which were concentrated on the anterior and lateral surfaces of the vertebral bodies, with the anterior–superior margins of the vertebrae being unaffected (Figs. 1 and 2). Such lesions are consistent with various disease processes, including TB and brucellosis. Burial 2272 displayed cavitating lytic lesions in the vertebral bodies of T3–T12 and L1, L2, and L4. The lesions ranged in size from 0.75–9.16 mm high, 0.39–9.78 mm wide, and 3.66–10.01 mm deep. Columns of trabecular bone ran cranial to caudal with the larger lesions (Fig. 3a). Rib fragments displayed cortical expansion and macroporosity on the parietal surface of the rib beginning at the rib angle and continuing anteriorly. Sclerotic bone was present at the femoral necks and just superior to the condyles on the posterior surfaces of both femora. The femora and tibiae diaphyses were also affected by periostitis.

Burial 4015 displayed cavitating lytic lesions on the anterior surface of the vertebral bodies of T3–L2. The lesions were 2.62–9.06 mm high, 2.8–5.32 mm wide, and 4.33–11.75 mm deep. Like 2272, columns of trabecular bone running cranial to caudal were visible within the larger lesions (Fig. 3b). Several ribs also displayed cortical thickening and trabecular expansion. Porosity was present on the parietal surface of some rib fragments. Sclerotic bone was present on the posterior surface of the femora just superior to the distal epiphysis. The osteological results for the skeletal material included in the molecular analysis are summarized in Table 1.

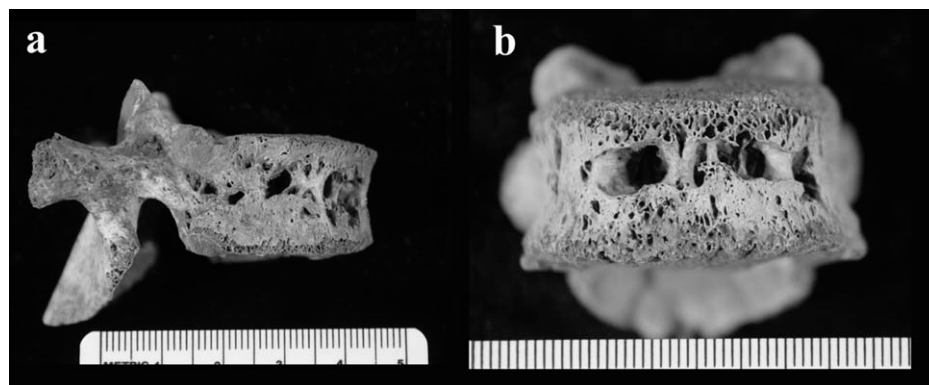


Fig. 3. Close-up of affected vertebrae. (a) Right lateral aspect of T9 from Butrint Burial 2272; (b) anterior aspect of T10 from Butrint Burial 4015.

Molecular analyses

PCR amplification and sequencing of mtDNA. HVI was successfully amplified from vertebrae, ribs, and long bone of all skeletons harboring pathologies, showing that viable DNA remained in the skeletal material. On average, 100–150 bases of forward and reverse sequence were obtained from bones of Burials 213, 319, 2272, and 5010. Burial 4015's vertebra, rib, and femur generated HVI PCR product, however, readable sequence was only obtained from the femur and rib. Each skeleton produced a unique mtDNA haplotype (Table 2).

PCR amplification of MTB complex and *Brucella* spp. DNA. Repeated attempts at amplifying TB markers *IS6110* insertion element, *oxyR* pseudogene, and *mtp40* gene were negative for all bones. In contrast, DNA from 19th century skeletal remains previously shown to be

TABLE 2. mtDNA sequences for tested burials^a

	16059	16077	16078	16094	16199
CRS	A	A	G	T	T
Analyst		G		C	
Burial #					
213	—			C	A
319	—				A
2272				C	A
4015	—				
5010	T		A		

^a Sequence for each burial compared to the Cambridge Reference Sequence (Anderson et al., 1981). An empty box indicates that the individual contained the same base as the reference at that position. Gray boxes denote areas where sequence was not obtained for that individual. Note that each burial produced a unique haplotype, different from the analyst, indicating that viable DNA was present in each skeleton.

TB positive (Ubelaker and Jones, 2003) successfully amplified (data not shown), as did control MTB complex DNA, down to approximately one bacterial genome equivalent. Reagent blanks and negative controls did not amplify.

Subsequent testing for *Brucella* spp. DNA generated very different results. Control skeletons that had no skeletal pathology (Burials 10 and 584) along with those that had pathologies but did not show vertebral cavitating lytic lesions (Burials 213, 319, and 5010) generated no amplification products. In contrast, DNA from the two skeletons that had vertebral lesions (Burials 2272 and 4015) amplified. Specifically, *IS6501* real-time amplification for rib and vertebral DNAs from Burial 4015 was positive, as was rib DNA from Burial 2272. Further, *Bscp31* amplified from vertebra and rib DNAs of Burial 4015. Dissociation curves for these PCR products were concordant with control *Brucella* DNA (e.g., Fig. 4), whereas reagent blanks and negative controls showed no amplicons beyond primer-dimer. The size of the amplification products was confirmed by gel electrophoresis (Fig. 5).

***Brucella* spp. DNA sequencing results.** DNAs from ribs of the two individuals with vertebral lesions (Burials 2272 and 4015) produced amplicons following subsequent *IS6501* amplification using biotinylated reverse primers. DNA pyrosequences were obtained, and a BLAST search showed 100% homology with the *Brucella* spp. *IS6501* element. Further sequencing using forward biotinylated primers confirmed these results.

DISCUSSION

In this study, osteological and molecular methods were used to confirm brucellosis infection as the cause of cavitating circular lytic vertebral lesions in ancient skeletal remains from Butrint, Albania. Skeletal lesions were

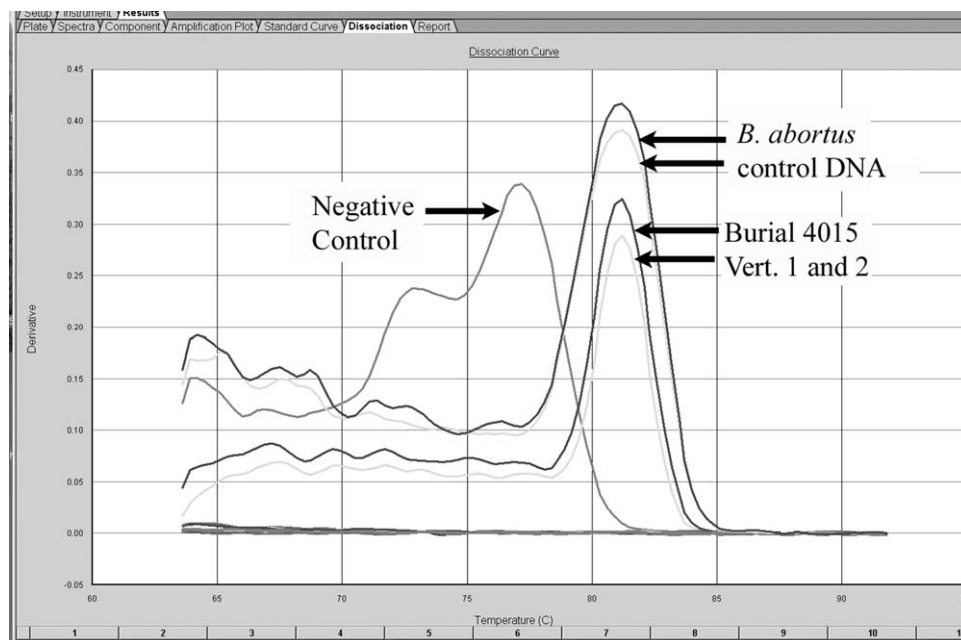


Fig. 4. *IS6501* real-time PCR dissociation curve of Burial 4015 vertebra (Vert.) and *B. abortus* DNA. The y-axis indicates changes in the relative fluorescence units (derivative of the rfu) as the temperature (°C) was ramped from 64°C to 95°C (x-axis). The apex of the curve indicates the melting temperature of the PCR products. Note that bone DNA product had the same melting profile as *B. abortus* control DNA, whereas the negative control (which showed some amplification in this assay) was inconsistent, representing primer dimer production.

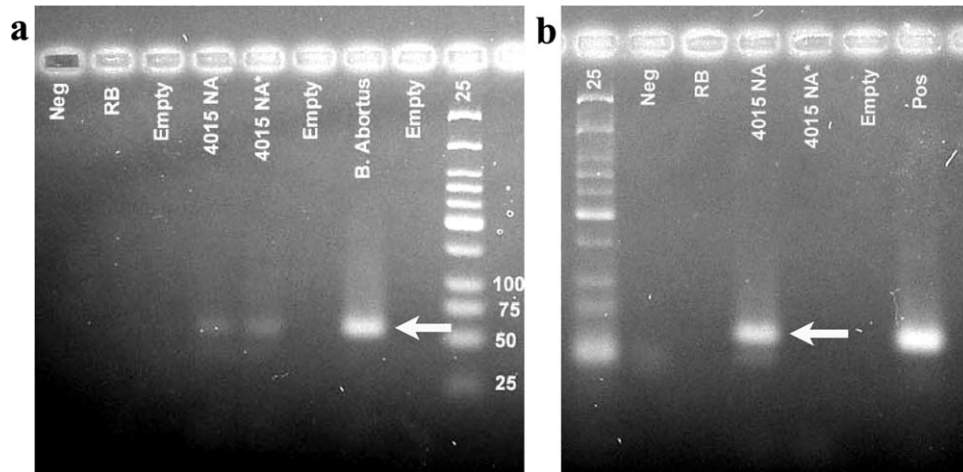


Fig. 5. Agarose gel electrophoresis of real-time PCR products from Burial 4015 vertebra DNA. Reactions from bone and *B. abortus* positive control DNA produced consistent products, indicated by the arrows (*: 1–10 DNA dilution; NA: the vertebral body was sampled proximal to the neural arch; 25: a 25 base pair ladder). (a) Products obtained while screening for the 58 bp multicopy IS6501 element; (b) product obtained while screening for the 59 bp Bsp31 gene. Primer dimer was observed in some negative control (Neg) and reagent blanks (RB) reactions.

first examined using osteological methods to generate a list of causative agents through differential diagnoses. DNAs from these remains were then extracted, and molecular techniques were used to confirm that genomic material from *Brucella* spp. was present. Through combined anthropological and molecular findings, this study demonstrates a verified occurrence of brucellosis infection in ancient remains from the Mediterranean Basin.

To date, there is no established osteological method for diagnosing *Brucella* spp. infection in human skeletal material. Some authors (e.g., Anderson, 2003) have cited spondylitis and vertebral marginal lysis as markers of the disease. Other osteological studies have examined extra-vertebral involvement. Soulié (1982) utilized joint and long bone abnormalities as indicators of brucellosis, whereas Capasso (1999) focused on rib lesions associated with antero-superior angling of the vertebral body. Further, Ortner (2003) described cavitating lytic lesions on the anterior aspect of vertebral bodies as resulting from *Brucella* spp. infection. However, all of these were presumed, not validated cases of brucellosis.

Ambiguity regarding skeletal involvement in brucellosis has extended into clinical studies. Most clinical literature places emphasis on the radiological signs first recognized by Pedro-Pons, wherein brucellosis is identified through spondylitis in the lumbar region, followed by sclerosis along the vertebral margins and a narrowing of the intervertebral disk space (Lifeso et al., 1985). Karabay et al. (2007) diagnosed cases of brucellosis using this methodology and it has become generally accepted. In spite of this, clinical studies comparing TB and brucellosis patients have shown that both diseases can generate the Pedro-Pons' sign (e.g., Cordero and Sanchez, 1991), and thus it is not likely a confirmatory indicator of *Brucella* spp. infection. Similarly, it has been noted that clinical methods used to identify spinal brucellosis do not translate well to dry, ancient skeletal materials (Etxebarria, 1994; Curate, 2006).

Interestingly, the skeletons at Butrint, which were verified as infected by *Brucella* spp. utilizing molecular techniques, shared very few of the characteristics

detailed above. The parrot-beak osteophytes and the radiological Pedro-Pons' sign were absent from 2272 and 4015. Instead, these individuals prominently displayed cavitating lytic lesions on the anterior and lateral surfaces of the vertebral bodies, with minor rib or other bone involvement, although the ribs, along with vertebrae, did test positive for *Brucella* spp.

Differences in pathology descriptions between archaeological reports and modern clinical studies exemplify how little is known about the skeletal response to *Brucella* spp. infection. As a result, brucellosis is very difficult to diagnose differentially with confidence using traditional osteological methods. Uncertainties are exacerbated by the fact that other disease processes, skeletal abnormalities, and taphonomic changes can produce skeletal responses similar to brucellosis. For example, Mays (2007) doubted the reliability of anterior–superior epiphysitis on lumbar vertebrae as a distinct marker of brucellosis and warned that anterior disc herniation can produce the same pathology. He also reported that 4% of the Wharram Percy skeletal collection displayed vertebral marginal lesions, all of which molecularly tested positive for TB and negative for *Brucella* spp. The author stated that anterior disc herniation was the most likely explanation for the vertebral lesions in these samples and concluded that suspected cases of brucellosis should not be diagnosed without supporting molecular evidence.

Such discrepancies in skeletal brucellosis identification have led many researchers to emphasize the importance of using molecular methods in ancient DNA studies. However, although DNA analysis is a valuable tool in verifying osteological findings, it is not without limitations (O'Rourke, 2000; Pääbo et al., 2004; Donoghue, 2008). Ancient biological material is often subjected to harsh environmental conditions and exposed to a variety of microorganisms, which can result in postmortem degradation and chemical modifications of DNA. In addition, PCR amplification and subsequent analyses may be difficult due to variability in the extracted DNA quality and quantity. The molecular techniques utilized in this study were designed to overcome these limitations. DNA isola-

tions were repeated to ensure that results were reproducible. Further, multicopy loci were assayed, nested-PCR was utilized, amplicon sizes were small, and pyrosequencing allowed examination of these very small stretches of DNA. The combination of osteological and molecular methods used to analyze vertebrae and ribs of the two adolescent skeletons from Butrint Albania, including the successful amplification of the *Brucella* spp. *IS6501* and *Bscp31* loci, confirmed that brucellosis was the causative agent of the lesions on these remains, and represents the first published cases of brucellosis in ancient remains [Donoghue (2008) stated via personal communication that another group amplified *IS6501* from a Siberian Iron Age female skeleton that showed lytic vertebral lesions, which acts to confirm the utility of these markers for identification of brucellosis in ancient skeletal material].

The occurrence of brucellosis in ancient remains from Butrint, located in the Mediterranean basin, is intriguing, as archaeological evidence has suggested its presence in the Mediterranean and Europe from the Chalcolithic period through the 19th century (Anderson, 2003; Capasso, 1999). Even today countries such as Greece and Albania report the highest rates of brucellosis infection in Europe (Pappas et al., 2006). In this regard, subsequent osteological examinations in Butrint and Diaporit have uncovered seven more burials, dating from the 5th to 14th century, with cavitating lytic lesions on the anterior and/or lateral surfaces of thoracic and lumbar vertebral bodies, consistent with Burials 2272 and 4015. Rib porosity was apparent in four of these individuals, all of which suggest that brucellosis was a common occurrence in ancient Butrint and Diaporit, spread over many centuries.

Today, epidemiological studies of brucellosis show that it is usually acquired through ingestion of contaminated meat or dairy, or from regular contact with infected animals, as might be expected of herders of cattle or sheep (Wallach et al., 1997). The consumption of dairy products is the primary route of modern infection in childhood cases (El-Amin et al., 2001; Tsolia et al., 2002), and studies in areas with endemic brucellosis indicate that children and young adults represent 20–70% of the cases (Gotuzzo et al., 1982; Mantur et al., 2004). Further, the regional diets of countries surrounding the Mediterranean basin have included yogurt, soured milk, and fresh cheeses since ancient times (Stambaugh, 1988). Individuals in these societies may have consumed contaminated dairy products or lived in close proximity to infected animals without realizing the risk of zoonotic infection. In 1999, Capasso attempted to show a correlation between dairy products and brucellosis in the ancient city of Herculaneum. Several individuals at the site harbored potential brucellosis derived pathologies. Subsequently, scanning electron microscopy of preserved cheese revealed bacteria consistent in morphology with *Brucella* spp., although attempts at molecular identification were unsuccessful (Capasso, 2002). In the current study, skeletal and molecular analyses clearly showed the presence of *Brucella* spp. infection in ancient Butrint, which, as today, occurred in young individuals. The severity of the vertebral lesions, and the ability to detect pathogen DNA, indicate that these individuals were in advanced stages of infection at the time of death, and suggests that exposure to the bacterium likely occurred at an early age through diet or childhood chores, such as caring for livestock.

Finally, it is worth noting that the period to which the remains date (10–13th centuries) corresponds to the era just prior to the revitalization of Butrint, when the city was largely in ruins. At this time the ancient city had dwindled to a small town of timber buildings, likely surviving as a periodic market and fishing center, before being deserted by the Venetians for the opposite bank of the Vivari Channel in the late 16th century (Hodges, 2004). Livestock during the period, even those showing signs of disease, would have been a valuable commodity, and meat and dairy products from them would probably still have been consumed. Similarly, it seems possible that an association between livestock disease and human illness went unrecognized, particularly given the overall harsh conditions that had befallen Butrint and Diaporit. Through the data presented here, it is verified that brucellosis has been established in the region for a long period of time. These findings not only provide novel information about the people of ancient Albania, but also aid in the identification and description of the disease in other ancient societies.

LITERATURE CITED

- Acha P, Szyfres B. 1980. Zoonoses and communicable diseases common to man and animals. Washington, DC: Pan American Health Organization.
- Anderson S, Bankier AT, Barrell BG, deBruijn MHL, Coulson AR, Drouin J, Eperon IC, Nierlich DP, Roe BA, Sanger F, Schreier RH, Smith AJH, Staden R, Young IG. 1981. Sequence and organization of the human mitochondrial genome. *Nature* 290:457–465.
- Anderson T. 2003. The first evidence of brucellosis from British skeletal material. *J Paleopathol* 15:153–158.
- Applied Biosystems. 2006. SYBR green PCR master mix and RT-PCR reagents protocol. Foster City.
- Aufderheide AC, Rodriguez-Martin C. 1998. The Cambridge encyclopedia of human paleopathology. Cambridge: Cambridge University Press.
- Ariza J, Gudiol F, Valverde J, Pallarés R, Fernández-Viladrich P, Rufi G, Espadaler L, Fernández-Nogues F. 1985. Brucellar spondylitis: a detailed analysis based on current findings. *Rev Infect Dis* 7:656–664.
- Bowden W, Hodges R. 2011. The medieval occupation of the merchant's house. In: Bowden W, Hodges R, editors. *Butrint 3: excavations at the Triconch Palace*. Oxford: Oxbow. p203–208.
- Buikstra J, Ubelaker D. 1994. Standards for data collection from human skeletal remains. In: *Arkansas archaeological report research series no. 44*. Fayetteville: Arkansas Archeological Surveys. p40–44.
- Bricker BJ. 2002. PCR as a diagnostic tool for brucellosis. *Vet Microbiol* 90:435–446.
- Capasso L. 1999. Brucellosis at Herculaneum (79AD). *Int J Osteoarchaeol* 9:277–288.
- Capasso L. 2002. Bacteria in two-millennia-old cheese, and related epizoonoses in Roman populations. *J Infection* 45:122–127.
- Cordero M, Sanchez I. 1991. Brucellar and tuberculous spondylitis: a comparative study of their clinical features. *J Bone Joint Surg Br* 73:100–103.
- Curate F. 2006. Two possible cases of brucellosis from a Clarist monastery in Alacer do Sal, southern Portugal. *Int J Osteoarchaeol* 16:453–458.
- Donoghue H. 2008. Molecular palaeopathology of human infectious disease. In: Pinhasi R, Mays S, editors. *Advances in human palaeopathology*. Chichester: John Wiley & Sons Ltd. p147–176.
- El-Amin EO, George L, Kutty NK, Sharma PP, Choithramani RS, Jhaveri VP, Salil P, Bedair SM. 2001. Brucellosis in children of Dhofar Region, Oman. *Saudi Med J* 22:610–615.

- Etcheberria F. 1994. Vertebral epiphysitis; early signs of brucellar disease. *J Paleopathol* 6:41–49.
- Geyik MF, Gür A, Nas K, Cevik R, Saraç J, Dikici B, Ayaz C. 2002. Musculoskeletal involvement of brucellosis in different age groups: a study of 195 cases. *Swiss Med Wkly* 132:98–105.
- Glasgow MM. 1976. Brucellosis of the spine. *Br J Surg* 63:283–288.
- Gotuzzo E, Alarcón GS, Bocanegra TS, Carrillo C, Guerra JC, Rolando I, Espinoza LR. 1982. Articular involvement in human brucellosis: a retrospective analysis of 304 cases. *Semin Arthritis Rheum* 12:245–255.
- Hershkovitz I, Donoghue HD, Minnikin DE, Besra GS, Lee OY-C, Gernaey AM, Galili E, Eshed V, Greenblatt CL, Lemma E, Bar-Gal GK, Spigelman M. 2008. Detection and molecular characterization of 9000-year-old *Mycobacterium tuberculosis* from a Neolithic settlement in the eastern Mediterranean. *PLoS ONE* 3:1–6.
- Hodges R. 2004. Byzantine Butrint: concluding remarks. In: Hodges R, Bowden W, Lako K, editors. *Byzantine Butrint: excavations and surveys 1994–1999*. Oxford: Oxbow. p321–326.
- Integrated Archaeological Database. 2011. Butrint Foundation-Albania. Available from: <http://www.iadb.co.uk/butrint/> [Accessed 28 September 2011].
- Işcan MY, Loth SR, Wright RK. 1984. Metamorphosis at the sternal rib end: a new method to estimate age at death in white males. *Am J Phys Anthropol* 65:147–156.
- Işcan MY, Loth SR, Wright RK. 1985. Age estimation from the rib by phase analysis: white females. *J Forensic Sci* 30:853–863.
- Karabay O, Gurel K, Sirmatel O, Sirmatel F. 2007. Brucellar spondylitis (Pedro-Pons' sign). *New Zeal Med J* 120: 97–99.
- Kelly PJ, Martin WJ, Schirger A, Weed LA. 1960. Brucellosis of the bones and joints: experience with 36 patients. *J Am Med Assoc* 174:347–353.
- Lifeso RM, Harder E, McCorkell SJ. 1985. Spinal brucellosis. *J Bone Joint Surg Br* 67:345–351.
- Lovejoy CO, Meindl RS, Pryzbeck TR, Mensforth, RP. 1985. Chronological metamorphosis of the auricular surface of the ilium: a new method for the determination of skeletal age at death. *Am J Phys Anthropol* 68:15–28.
- Mantur BG, Akki AS, Mangalgi SS, Patil SV, Gobbur RH, Peerapur BV. 2004. Childhood brucellosis—a microbiological, epidemiological, and clinical study. *J Tropical Pediatr* 50:153–157.
- Mays S. 2007. Lysis at the anterior vertebral body margin: evidence for brucellar spondylitis? *Int J Osteoarchaeol* 17:107–118.
- Mays S, Taylor GM, Legge AJ, Young DB, Turner-Walker G. 2001. Paleopathological and biomolecular study of tuberculosis in a medieval skeletal collection from England. *Am J Phys Anthropol* 114:298–311.
- Mays S, Fysh E, Taylor GM. 2002. Investigation of the link between visceral surface rib lesions and tuberculosis in a medieval skeletal series from England using ancient DNA. *Am J Phys Anthropol* 19:27–36.
- Ortner DJ. 2003. Identification of pathological conditions in human skeletal remains. San Diego: Academic Press.
- O'Rourke DH, Hayes MG, Carlyle SW. 2000. Ancient DNA studies in physical anthropology. *Annu Rev Anthropol* 29:217–242.
- Ouahrani S, Michaux S, Sri Widada J, Bourg G, Tournebize R, Ramuz M, Liautard JP. 1993. Identification and sequence analysis of IS6501, an insertion sequence in *Brucella* spp.: relationship between genomic structure and the number of IS6501 copies. *J Gen Microbiol* 139:3265–3273.
- Pääbo S, Poinar H, Serre D, Jaenicke-Despres V, Hebler J, Rohland N, Kuch M, Krause J, Vigilant L, Hofreiter M. 2004. Genetic analyses from ancient DNA. *Annu Rev Genet* 38:645–679.
- Pappas G, Papadimitriou P, Akritidis N, Christou L, Tsianos, EV. 2006. The new global map of human brucellosis. *Lancet Infect Dis* 6:91–99.
- Phenice TW. 1969. A newly developed visual method of sexing the os pubis. *Am J Phys Anthropol* 30:297–301.
- Raoult D. 2008. Molecular detection of past pathogens. In: Raoult D, Drancourt M, editors. *Paleomicrobiology*. Berlin: Springer. p55–68.
- Scheuer L, Black SM. 2004. *The juvenile skeleton*. London: Elsevier Academic Press.
- Sharif HS, Aideyan OA, Clark DC, Madkour MM, Aabed MY, Mattsson TA, al-Deeb SM, Moutaery KR. 1989. Brucellar and tuberculous spondylitis: comparative imaging features. *Radiology* 171:419–425.
- Soulié R. 1982. Brucellosis: a case report dating from 650–700AD. *Palaeopathol Newsl* 38:7–10.
- Stambaugh J. 1988. *The ancient Roman city*. Baltimore: The John Hopkins University Press.
- Steinbock RT. 1976. *Paleopathological diagnosis and interpretation: bone diseases in ancient human populations*. Springfield, IL: Charles C. Thomas.
- Suchey JM, Katz D. 1998. Applications of pubic age determination in a forensic setting. In: Reichs K, editor. *Forensic osteology: advances in the identification of human remains*. Springfield, IL: Charles C. Thomas. p204–236.
- Tsolia M, Drakonaki S, Messaritaki A, Farmakakis T, Kostaki M, Tsapra H, Karpathios T. 2002. Clinical features, complications and treatment outcome of childhood brucellosis in central Greece. *J Infect* 44:257–262.
- Turunc T, Demiroglu YZ, Uncu H, Colakoglu S, Arslan H. 2007. A comparative analysis of tuberculosis, brucellar, and pyogenic spontaneous spondylodiscitis patients. *J Infect* 55:158–163.
- Ubelaker DH. 1984. *Human skeletal remains: excavation, analysis, interpretation*. Revised edition. Washington, DC: Taraxacum.
- Ubelaker DH, Jones EB, ed. 2003. *Human remains from Voegtly Cemetery, Pittsburgh, Pennsylvania*. Smithsonian Contributions to Anthropology Series, Number 46. Washington, DC: Smithsonian Institution Press.
- Uhlinger E. 1970. Die Pathologische Anatomie der Hamatogenen Osteomyelitis. *Der Chirurg* 41:193–198.
- United Nations Educational, Scientific And Cultural Organization (UNESCO). 1999. *Butrint Albania: Advisory Board Evaluation*. Available from: http://whc.unesco.org/archive/advisory_body_evaluation/570bis.pdf [Accessed 19 September 2011].
- Wallach JC, Samartino LE, Efron A, Baldi PC. 1997. Human infection by *Brucella melitensis*: an outbreak attributed to contact with infected goats. *FEMS Immunol Med Microbiol* 19:315–321.